

Effect of aggregate type on the fatigue durability of asphalt mixtures

G. Valdés-Vidal^{a,*}; A. Calabi-Floody^a; E. Sanchez-Alonso^a; R. Miró-Recasens^b

^a Department of Civil Engineering, Universidad de La Frontera, Temuco, Chile

^b Department of Civil Engineering, Technical University of Catalonia, Barcelona, Spain.

Abstract: Effect of aggregate type on the fatigue behaviour of asphalt mixture is an important variable to ensure greater durability of the pavements over time. This study presents the main results about the evaluation of the physical properties of different aggregates on the fatigue behaviour of asphalt mixtures. Two fatigue tests were used for this study, one standardized and another, which was recently developed and evaluates dissipated energy during the cracking process of the asphalt mixtures (EBADE[®] test). Three types of aggregates were used and adjusted to a semi-dense aggregate gradation: two of fluvial type (AF1 and AF2) and one from quarry (AC). Two different shredding processes were used to obtain them. The results obtained show that there is a greater relationship between the shape and texture of the fine aggregates and the fatigue behaviour of the mixtures. It was also showed that the greater the thickness of the mixture in the pavement structure, the more influence these properties have. Likewise, the shape and texture properties of the fine aggregate influence the ability of asphalt mixtures to dissipate energy during the process of fatigue damage.

Keywords: aggregates, shape, texture, EBADE[®] test, stiffness, fatigue, durability

*Corresponding author.
E-mail addresses: gonzalo.valdes@ufrontera.cl
Telephone contact: (+56-45) 259.65.33

26 1. INTRODUCTION

27 Most of the roads and highways are built with asphalt mixtures due to they provide good mechanical
28 properties, smoothness and durability [1]. However, the performance of asphalt mixtures are conditioned to
29 environmental conditions, traffic loads and mainly, the properties of their materials (mineral aggregates,
30 asphalt binder and filler) [2]. In relation to the aggregates, their properties (physical and mineralogical) can
31 affect the mechanical behavior of an asphalt mixture. In this context, one of the main damages that affect
32 asphalt pavements is fatigue cracking [3, 4], which is the reason why the study of this phenomenon has
33 become a fundamental aspect to consider in the durability of pavements [5]. A material becomes fatigued
34 when it cracks as a result of the accumulation of individual repeated loads whose magnitudes are below the
35 ultimate strength of the material [6]. Numerous efforts have been made to understand the phenomenon of
36 fatigue in asphalt mixture. This phenomenon is evaluated in laboratories through different standardized
37 methods which are based on reproducing the state of stress that occurs in the layer subjected to traffic [3, 7].
38 These methods involve a long implementation period and are characterized by subjecting different types of
39 asphalt specimens to cyclic loading applications, in which the applied deformation or tension is maintained
40 constant until the failure of the mixture takes place. The traditional criterion of fatigue failure of standardized
41 trials is the 50% reduction in stiffness [8- 10]. However, other researchers consider that the dissipated energy
42 in the fracture process is an indicator of a better fatigue performance of the mixture. When there is a higher
43 quantity of energy dissipated in the fracture process, this is considered an indicator of a better fatigue
44 performance of the asphalt mixture [11-14]. The EBADE[®] test developed in the laboratory of the Technical
45 University of Catalonia, is a new test which incorporates dissipated energy in the fracture process as a
46 measurable variable. By using this test method, research already carried out conclude that asphalt mixtures
47 with more dissipated energy in the cracking process require more energy to break the mixture and therefore
48 show a better fatigue behaviour [14].

49 On the other hand, asphalt mixtures correspond to a composite material whose matrix is usually composed
50 approximately of 5% asphalt binder and 95% aggregates; consequently, the influence of aggregates on the
51 performance of the asphalt mixture is very important [15]. Pan et al. [16] have shown that there is a good
52 correlation between the properties of the aggregates specified by the SHRP and the mechanical behaviour of
53 the asphalt mixtures. In this context, Aragão et al. [17] indicated that the characteristics of the coarse

54 aggregates correlated better with the resistance to the damages evaluated. The authors also concluded that the
55 superficial texture of the particles showed a strong correlation with the performance of the asphalt mixtures
56 and recommended including this parameter in the specifications of asphalt mixture design. Hu et al. [15]
57 demonstrated that particle size was related with the deformations that occurred in the asphalt mixture,
58 indicating that if the size of the particles increases, the deformations in the mastic do as well. Other authors
59 have pointed out that the properties of the asphalt mixture both during the compaction process and in service
60 are influenced by the geometric characteristics of the aggregates, thereby indicating that the particle size,
61 shape index and the angularity of the aggregates are factors to be considered in this order of importance [18].
62 On his behalf, Aragão et al. [17] showed that the modulus of stiffness, especially at intermediate and low
63 frequencies, is affected by the morphological characteristics of the aggregates. In recent years, the study of the
64 morphological properties of aggregates through image analysis techniques has gained relevance; a few
65 examples of this are Computer Particle Analyzer, Video Imaging System (VIS), Camsizer, Wipshape,
66 Aggregate Imaging System (AIMS) [17]. By using image analysis technologies, Sukhwani et al. [19]
67 determined an angularity and texture gradient, whereby they predicted that granitic aggregates possess an
68 elevated texture and consequently may show better adherence characteristics with asphalt binder, compared to
69 limestone aggregates which showed lower angularity and texture gradients. Zhang et al. [20] defined an index
70 that combines the effects of angularity and texture in coarse aggregates; this index would be beneficial as an
71 aggregate selection parameter. Other studies have demonstrated that the physical parameters of the aggregates
72 such as the Particle Index determined by the method proposed by the ASTM-D3398, as well as the shape
73 parameters proposed by Zingg [21], showed interesting correlations in regard to the stiffness and resistance to
74 cracking at low temperatures [22], and the adhesion and cohesion properties of aggregate-binder matrix [23].
75 As noted above, it has been revealed that getting to know how the physical and morphological characteristics
76 of aggregates influence the fatigue performance of an asphalt mixture through simple procedures, would
77 allow to design and select more efficient asphalt mixtures in fatigue performance. Through this design and
78 selection, the hope is to contribute to the creation of more resistant asphalt mixtures.

79 This study shows the influence of aggregate type on the fatigue resistance of asphalt mixtures. Three types of
80 aggregates have been studied which differ from each other by their physical, morphological and mineralogical
81 characteristics. The fatigue performance of the asphalt mixtures have been evaluated through a standardized

82 test method and a new test procedure (EBADE[®]), whereby the dissipated energy in the fracture process of the
83 asphalt mixtures have been evaluated. Additionally, the results of the effect of aggregate shape and texture
84 properties on pavement structure durability are presented, defined through a fatigue life analysis given by a
85 mechanistic-empirical design methodology.

86

87 **2. MATERIALS AND METHODS**

88 **2.1 Materials**

89 The asphalt binder used in this study was a CA24 conventional binder whose characterization in accordance
90 with Chilean standard is showed in Table 1.

91 Three types of aggregates were evaluated; two of fluvial origin, AF1, and AF2 and one of quarry origin AC.
92 AF1 and AF2 differ in terms of their shapes, due to the production process. AF1 and AC, whose particles are
93 more irregular, were obtained through a final cone crushing process, while AF2 was obtained through a final
94 impact crushing process, Figure 1.

95 AF1 and AF2 were extracted from the same source and are mainly composed of the particles dolomite, basalt,
96 dacites, andesites, rhyolites, sandstone, quartz, and quartzite. The quarry aggregate, AC, is primarily
97 composed of quartz, biotite and iron oxides. A chemical analysis of the aggregates was performed using
98 Scanning Electron Microscopy (SEM). It was observed that both the quarry aggregate and the fluvial
99 aggregates are of quartz type and their average silica content corresponds to 59.9% for AF1, 59.1% for AF2
100 and 63.3% for AC.

101 The aggregates were characterized for their use in an asphalt mixture, Table 2. The average size measurement
102 of the filler particles was performed through an image analysis by using the light scattering phenomenon. This
103 methodology acts through the alteration of the direction and intensity of a beam of light that strikes an object
104 due to the combination of reflection, refraction, and diffraction. The average values of the particles obtained
105 were 708nm for AF1, 298nm for AF2 and 351nm for AC.

106 The morphology of the aggregates was determined by the Zingg method, which it corresponds to a procedure
107 that classifies different particles of coarse aggregates according to their shape [21]. This method is based on
108 the measurement of length, width and thickness of particles greater than 5 mm in order to obtain four
109 parameters: shape factor, sphericity factor, elongation ratio and flatness ratio according to the equations

110 described in the protocol [21]. With the elongation and flatness relationships, four aggregate shapes are
111 defined: disk, rod, cubical, and blade. Table 3 shows values of the three types of aggregates according to
112 Zingg method, classifying as laminar for the aggregate AC, disk-like for AF1, and cube-like for AF2.

113 Particle shape and texture characterization were obtained according to Particle Index (PI), determined by the
114 ASTM-D3398 standard. PI is a parameter that represents a global measurement of the shape and texture
115 characteristics of aggregates. PI values were calculated in accordance with this standard (Criterion I) as well
116 as with two different criteria defined to this study (Criterion II and III) to explain the phenomenon observed in
117 the mechanical performance of the mixtures. The criteria used for the calculation of the PI and its results are
118 described in Table 4.

119 2.2 Mixtures design

120 A semi-dense asphalt mixture was selected according to Chilean Standards, with a maximum aggregate size
121 of 12.5 mm (Table 5). An optimal asphalt binder content of 5.2% on weight of aggregates was obtained using
122 the Marshall method. This optimal binder content was used in the three asphalt mixtures manufactured (AF1,
123 AF2 and AC). The mixing and compaction temperatures were 155°C and 145°C, respectively.

124 2.3 Test methods

125 The fatigue laws of each asphalt mixture were determined by applying the procedure described in the standard
126 UNE-EN 12697-24, Annex E. Cylindrical specimens were used to characterize the behaviour of the asphalt
127 mixtures by subjecting them to repeated diametral compression loading. The deformations produced in the
128 direction perpendicular to the load were registered. The test was performed at a temperature of 20°C with a
129 loading frequency of 10 Hz and stress levels of 200, 250 and 300 kPa. The failure criteria selected was
130 defined as the necessary loading cycle when the deformation reached twice its initial value, obtained in cycle
131 100. The deformation for each load application is calculated by applying Equation 1.

$$132 \quad \varepsilon_0 = \left[\frac{2\Delta H}{\Omega} \right] \chi \left[\frac{1+3\nu}{4+\pi\nu-\pi} \right] \quad (1)$$

133 Where, ε_0 is the tensile strain in the center of the sample in ($\mu\epsilon$), ΔH the total horizontal deformation in (mm),
134 Ω is the diameter of the sample in (mm) and ν is the Poisson ratio.

135 To obtain the fatigue law of the asphalt mixture, the value pairs were considered: initial deformation and
136 failure cycle for each of the tested load amplitudes. Lastly, using a least-squares approach, the fatigue law is
137 obtained using Equation 2.

138
$$\varepsilon = a \cdot N^{-b} \quad (2)$$

139 Where ε is the tensile strain, N is the number of strain applications to failure; a , b are the fatigue growth rate
140 coefficients.

141 For each fatigue law (AF1, AF2 and AC), 18 cylindrical fatigue samples were manufactured by gyratory
142 compactor (diameter 100 mm) applying the same compaction energy (100 cycles at 600kPa and 0.82°). For
143 each stress level evaluated, the average value of six samples was calculated.

144 The stiffness modulus has been determined by indirect tensile strength (ITS) test described in the standard
145 UNE-EN 12697-26, Annex C. This methodology consists of applying a sinusoidal pulse loads and periods of
146 rest to produce a controlled horizontal deformation in cylindrical specimens. The stiffness modulus is
147 obtained by applying Equation 3.

148
$$S_M = \frac{F \cdot (v+0.27)}{(z \cdot h)} \quad (3)$$

149 Where S_M is the stiffness modulus measured in (MPa), F is the maximum vertical load in (N), z is the
150 amplitude of horizontal deformation in (mm), h is the average thickness of the specimen in (mm), and v is the
151 Poisson ratio.

152 For each type of mixture, five cylindrical samples (diameter 100 mm) were manufactured by gyratory
153 compactor applying the same compaction energy (100 cycles at 600kPa and 0.82°). The test was performed at
154 20°C.

155 The EBADE® test was used to determine the dissipated energy in the fracture process of the asphalt mixtures
156 during the development of fatigue damage. This test consists of performing a scan for deformations in a cyclic
157 tension-compression test over a prismatic specimen, where two notches were made in the central area to
158 reduce the area of the specimen in the middle section in order for failure to take place, Figure 2a. To carry out
159 the EBADE® test, five cylindrical samples were manufactured for each asphalt mixture (AF1, AF2 and AC),
160 and compacted with the Marshall compactor applying 75 blows per face. The samples were cut to get the
161 dimensions according to the test method proposed by laboratory of the Technical University of Catalonia
162 [14]. The specimen dimensions were 6 cm of height and 5 cm in width and thickness. The specimens were
163 subjected to an increasing series of 5000 tension-compression stress cycles at 10 Hz and a temperature of 20
164 °C. The first series of cycles were initiated with a deformation of $2.5 \cdot 10^{-5}$ and the amplitude deformations
165 were increased in increments of the same value until the material broke, Figure 2b [14]. During the test, the

166 load and deformation produced were registered. In this way, parameters such as stress (σ), strain (ε), norm of
167 the complex modulus ($|E^*|$), and the dissipated energy density (DED) can be obtained. Norm of the complex
168 modulus was determined according to Equation 4.

$$169 \quad |E^*| = \frac{\sigma_{max}}{\varepsilon_{max}} \quad (4)$$

170 Where σ_{max} is the stress amplitude in a cycle and ε_{max} is the strain amplitude during the same cycle.

171 DED was calculated by adding the areas by cycle of the ellipse, which is formed in the load/displacement
172 graph, due to the delay between both signals by using the Gauss area formula according to Equation 5.

$$173 \quad DED = \frac{g}{S} \cdot \frac{1}{2} |(\sigma_1 \varepsilon_1 + \sigma_2 \varepsilon_2 + \dots + \sigma_{n-1} \varepsilon_{n-1} + \sigma_n \varepsilon_1) - (\sigma_2 \varepsilon_1 + \sigma_3 \varepsilon_2 + \dots + \sigma_n \varepsilon_{n-1} + \sigma_1 \varepsilon_n)| \quad (5)$$

174 Where g is gravity, S is the fracture area, $\sigma_i \varepsilon_i$ are the n values obtained from the load-displacement pairs for
175 each cycle.

176 **2.4 Evaluation of durability of asphalt mixtures**

177 To model the behaviour of the pavement structures in the face of the traffic loads, a mechanistic-empirical
178 pavement analysis was performed. The deformations were evaluated at critical points for different thicknesses
179 of proposed pavements for each mixtures studied in the experimental phase. The input variables were the
180 stiffness modulus of the asphalt layer obtained experimentally, the Poisson ratio and the thickness for each
181 layer that make up the structure. The structures analyzed are composed of an asphalt mixture of variable
182 thickness ranges from 10 to 30 cm, a granular base of 15 cm and a granular subbase of 15 cm supported over
183 the subgrade. The modules used for the granular base layers, granular subbase and subgrade were 279, 146
184 and 77 MPa, respectively.

185 In the durability analysis, two load configurations were used: a standard axis of 8.16 Tn of weight equivalent
186 to 80kN, used in mechanistic methods for the design of pavements; and a single axis double rotor of 11 Tn
187 weight equivalent to 110kN, which is the maximum weight allowed in Chile for this type of axis. The failure
188 criterion considered corresponds to fatigue cracks which are produced due to traction in the bottom of the
189 asphalt layer.

190

191 3. ANALYSIS OF THE RESULTS

192 3.1 Evaluation of fatigue behaviour and durability of the mixtures

193 The values obtained for the stiffness modulus test for the aggregates AC, AF1, and AF2 were 3153, 3791 and
194 3464 MPa, respectively. The results obtained do not show a clear relationship between the stiffness modulus
195 and the PI values of criteria I and II (Table 4). However, there is a correlation with the results of the weighted
196 PI of fine aggregates (criterion III) and the filler size, since, at a greater PI value and size value, the stiffness
197 modulus becomes greater. From this, it can be deduced that the shape and texture of the fine aggregates have
198 an influence on the stiffness of the mixtures; in other words, the more texture and angularity of aggregate the
199 more internal friction, giving greater modulus values.

200 In Figure 3 the fatigue laws of the evaluated mixtures are shown. The tested mixtures show similar laws of
201 fatigue; however, the fluvial aggregates showed a lower slope in the fatigue line than the AC mixtures, which
202 implies that these are less sensitive to deformation, as pointed out by Silva et al. [24]. This finding is related
203 to the results obtained in the stiffness modulus, as the mixtures that possess a greater modulus are mixtures
204 that are less susceptible to deformation for similar load values [25].

205 Taking into account the shape and texture of the aggregates using the PI value, a relationship with the
206 criterion III is observed, which, similar to the stiffness, the greater value of this index, the lower the slope of
207 the fatigue law is. In other words, the greater the texture and angularity of the fine aggregates are, the better
208 the behaviour of the mastic is. This better behaviour allows the internal friction in the mixture to be improved,
209 thus making it less susceptible to deformations.

210 In Figure 4 it can observe the results of the pavement structure durability with thicknesses from 10 to 30 cm
211 for the different mixtures evaluated according to the type of aggregate used; and for axis with 80 kN and 110
212 kN. In accordance with the results obtained, the deformations produced for each kind of mixture by the axis
213 110 kN are superior to those of 80kN; for this reason, their durabilities are less for the evaluated thicknesses.
214 However, the difference in durability between the different mixtures and the different thicknesses is lower in
215 the case of the axis of 110kN than for 80kN, as it can be observed in Table 6.

216 For both axle loads, it was proven that for a thickness layer of 10 cm there are no major differences in terms
217 of the durability of the mixtures among themselves. On the other hand, starting at 15 cm of thickness

218 important variations begin to be seen. From here, in all of the cases, the AF1 are the asphalt mixtures that
219 show the greatest durability, followed by AF2 and lastly, AC.

220 According to the ASTM-D3398 standard, the aggregates with a $PI \geq 15$ are classified as crushed particles
221 possessing high angularity. Due to the results obtained for the evaluated mixtures and the layer thicknesses
222 greater than 10 cm, the mixtures with particles containing a greater PI of fine aggregate (AF1 and AF2) prove
223 to be durable. This finding concurs with the study carried out by Kim et al. [26] who evaluated the mechanical
224 behaviour of the asphalt mixtures by analyzing the influence of the type of aggregate and its gradation,
225 changing the content, % voids and the temperatures; they also performed a statistical analysis to see the
226 principal effects and interactions. They concluded that the type of aggregate has a significant impact on both
227 properties evaluated; thereby allowing the mixtures with aggregates possessing a rough and angular texture, to
228 obtain a better performance, especially in permanent deformations.

229 At the same time, the mixture with more significant content of flakiness particles (AC) (Table 1), shows a
230 lower durability against the mixtures AF1 and AF2, due to the fact that when they possessed a greater amount
231 of flakiness, these tend to break during production and compaction. As a result, the probability of cracks
232 appearing increases and this results in fatigue failure in the pavement structure; this agrees on the studies
233 performed by Kandhal and Park [27] and González and Velandia [28]. These results may also be correlated
234 with aggregates' resistance to fragmentation since the aggregates which have demonstrated to be less resistant
235 in the Los Angeles test (Table 1), are those which have shown the worst results in durability. This fact
236 coincides with Moreno et al. [29] pointed out, where the most resistant aggregates showed a better behaviour
237 against cracking.

238 This behaviour could try to explain through the chemical composition of the aggregates, especially the silica
239 content, which indicates how acid the aggregate is, and how affects the adhesiveness of the mixture [30]. The
240 lowest amount of silica in the fluvial aggregates (AF1 and AF2 \approx 59%), with regard to the quarry aggregate
241 (AC \approx 63%), would influence a better adherence with the binder, showing a greater durability against fatigue
242 failure. However, this explanation could not be applied in analyzing the results of the mixtures with the fluvial
243 aggregates, since the AF2 aggregate shows a slightly lower acidity than AF1; therefore, they would have to
244 show a greater durability, Figure 4. Thus, in this case, it can be deduced that the shape, texture, and angularity

245 of the aggregates have more influence, correlated with the PI, than the chemical composition of the
246 aggregates.

247 **3.2 Dissipated Energy by EBADE® Test**

248 The results obtained in the EBADE® test for the 3 mixtures evaluated are shown in Figure 5 and Figure 6. The
249 evolution of the complex modulus ($|E^*|$) during the test is showed in Figure 5. These results indicate that the
250 mixture manufactured with the AF1 aggregate obtained the highest initial modulus value ($|E^*_i|$), 5851 MPa.
251 On the contrary, the value of $|E^*_i|$ of the mixture manufactured with AC obtained the lowest value, 2821 MPa;
252 and the mixture manufactured with the AF2 obtained an intermediate value. These findings are similar to
253 those reported for the ITS test, but the differences between them are greater. Also, all mixtures showed a
254 continuous and progressive damage as the strain level increased, without a sudden failure. In relation to Fig.
255 6, the dissipated energy during each cycle was recorded as the area of the hysteresis loop formed in the stress-
256 strain plane. In the initial stage, as the strain amplitude applied increased, so the stress amplitude did, and
257 consequently the hysteresis loop area and dissipated energy. In the second phase, once the asphalt mixture
258 reached its maximum stress amplitude, the dissipated energy gradually decreased, until the material failed.
259 AF1 and AF2 mixtures showed a greater accumulated dissipated energy density values (DED_a) in relation to
260 the AC mixture; 13,034,600 J/m³, 11,763,171 J/m³ and 4,769,555 J/m³, respectively. The DED_a by the AC
261 mixture was 63% lower than the DED_a by the AF1 mixture and 9.8% lower for the mixture AF2 against AF1.
262 These dates implies that in order to induce the same deformations in each cycle, AF1 mixture require more
263 work for each cycle, dissipating more energy throughout the whole fatigue process compared to the AF2 and
264 AC mixtures, being their fatigue resistance higher. Similarly to the previous section, these results appear to be
265 related with the PI of the fine aggregates, since the greater the PI of the fine aggregate, the more texture and
266 angularity the aggregates possess. As a result, mastic with a greater internal friction is formed, making them
267 more resistant to fatigue damage and giving them a greater capacity to support loads; this translates into a
268 greater capacity to dissipate energy during the fatigue process. As the same of previous fatigue analysis, it is
269 most important the shape, texture and angularity of the aggregates (PI value) than their chemical composition.
270 This could be explained, due to the little difference of percentages of silica, between 63% and 59%, classified
271 as intermediate acidic aggregate, according to Allen [30].

272 The EBADE® results obtained agrees on the results obtained in the study carried out by Valdés et al. [31], in
273 which cracking behaviour at low and intermediate temperatures was evaluated using the Fénix® test for the
274 same aggregates used in mixtures with four different binders. Those mixtures which showed a greater
275 resistance to cracking and greater flexibility capacity for similar stiffness values, were those mixtures
276 manufactured with the aggregates with greater values of texture and angularity of their fine aggregates,
277 similar to the results obtained in this study.

278 4. CONCLUSIONS

279 This study analyzed the influence of aggregate properties' on the deterioration of asphalt mixtures using the
280 standardized fatigue test, the EBADE® test and by studying the durability of pavement structures through the
281 analysis of the results of the mechanistic-empirical design method. The main conclusions obtained are:

- 282 • The shape and texture of the fine aggregates affect the stiffness, fatigue behaviour and durability of
283 the flexible pavement structures evaluated in this study.
- 284 • The asphalt mixtures with a greater PI value for the fine aggregates proved to be more rigid, less
285 susceptible to deformation and their durability increased with the greater the pavement thickness for
286 both types of axle loads evaluated, being lower in the case of 110kN for three types of aggregates
287 studied.
- 288 • The aggregates with greater PI value in the fine aggregate showed a more resistant behaviour to
289 fatigue cracking and a greater capacity to support loads, which translates into a greater capacity to
290 dissipate energy during the cracking process.
- 291 • For aggregates of the same origin, the shape and texture of the aggregate are important properties to
292 evaluate the fatigue behaviour.
- 293 • For aggregates of different origin, in addition to shape and texture, it is important to consider the
294 chemical nature of aggregates.
- 295 • The asphalt mixtures with a greater dissipated energy in the EBADE® test showed a better fatigue
296 behaviour.
- 297 • The EBADE® test allows evaluate the fatigue behaviour of the asphalt mixtures in a shorter time than
298 classical fatigue test; it also makes possible to see the effect of the properties of the aggregates on the
299 durability of the mixtures.

300 **5. ACKNOWLEDGMENTS**

301 The present paper is the result of the research supported by Universidad de la Frontera program, conducted
302 within the framework of the Project DI18-0053.

303 **6. REFERENCES**

- 304 [1] Asphalt Institute. (2007) The asphalt handbook (7th edition), ISBN: 978-1-934154-27-4.
- 305 [2] Teurquetil, F.; Raju, S. (2015) Chapter 11: Choosing asphalts for use in flexible pavement layers. The
306 Shell Bitumen Handbook, ICE Publishing, London. Pp. 261-293. ISBN: 978-0-7277-5837-8.
- 307 [3] Moreno, F.; Rubio, M. (2013) UGR-FACT test for the study of fatigue cracking in bituminous mixes.
308 Constr Build Mater 43, 184-190. <https://doi.org/10.1016/j.conbuildmat.2013.02.024>.
- 309 [4] Sadeq, M.; Al-Khalid, H.; Masad, E.; Sirin, O. (2016) Comparative evaluation of fatigue resistance of
310 warm fine aggregate asphalt mixtures. Constr Build Mater 109, 8-16.
311 <https://doi.org/10.1016/j.conbuildmat.2016.01.045>.
- 312 [5] Moreno-Navarro, F.; Rubio-Gámez, M.C. (2016) A Review of fatigue damage in bituminous mixtures:
313 Understanding the phenomenon from a new perspective. Constr Build Mater 113, 927-938.
314 <https://doi.org/10.1016/j.conbuildmat.2016.03.126>.
- 315 [6] Pérez, F.; Valdés, G.; Botella, R.; Miró, R.; Martínez, A. (2012) Approach to fatigue performance using
316 Fénix test for asphalt mixtures. Constr Build Mater 26, 372-380.
317 <https://doi.org/10.1016/j.conbuildmat.2011.06.036>
- 318 [7] Zhi, S.; Gun, W.W.; Hui, L.; Bo, T. (2012) Evaluation of fatigue crack behaviour in asphalt concrete
319 pavements with different polymer modifiers. Constr Build Mater 27, 117-125.
320 <https://doi.org/10.1016/j.conbuildmat.2011.08.017>.
- 321 [8] Hicks, R.G.; Finn, F.N.; Monismith, C.L.; Leahy, R.B. (1993) Validation of SHRP binder specification
322 through mix testing. Journal of the Association of Asphalt Paving Technologists, Asphalt Paving
323 Technology (AAPT) 62, 565-614. ISSN: 0270-2932.
- 324 [9] Williams, D. A. (1998) Microdamage healing in asphalt concretes: relating binder. Doctoral Thesis, Texas
325 A&M Univ., College Station, United States.

- 326 [10] Smith, B.; Hesp, S. (2000) Crack pinning in asphalt mastic and concrete: regular fatigue studies. *Transport*
327 *Res Rec* 1728, 75-81. Transportation Research Board. National Research Council. Washington, D.C.
328 <http://dx.doi.org/10.3141/1728-11>.
- 329 [11] Rowe, G. M. (1993) Performance of asphalt mixtures in the trapezoidal fatigue test. *Journal of the*
330 *Association of Asphalt Paving Technologists (AAPT)* 62, 334-384. ISSN: 0270-2932.
- 331 [12] Rowe, G. M.; Bouldin M. G. (2000) Improve techniques to evaluate the fatigue resistance of asphaltic
332 mixtures. *Proceedings of the 2nd Euroasphalt and Eurobitume Congress, Spain (2000)*. ISBN:
333 9080288438 9789080288430.
- 334 [13] Anderson, D.; Hir, Y.; Marasteanu, M.; Planche, J.-P.; Martin, D.; Gauthier, G. (2001) Evaluation of
335 fatigue criteria for asphalt binders. *Transport Res Rec* 1766, 48-56. Transportation Research Board.
336 National Research Council. Washington, D.C. <http://dx.doi.org/10.3141/1766-07>
- 337 [14] Pérez-Jiménez, F.; Botella, R.; Martínez, A.H.; Miró, R. (2013) Estimating the fatigue law of asphalt
338 mixtures using a strain sweep test (EBADE test). *5th EATA Conference, ISBS Institut für*
339 *Straßenwesen, Braunschweig*, 1-15.
- 340 [15] Hu, J.; Qian, Z.; Wang, D.; Oeser, M. (2015) Influence of aggregate particles on mastic and air-voids in
341 asphalt concrete. *Constr Build Mater* 93, 1-9. <https://doi.org/10.1016/j.conbuildmat.2015.05.031>.
- 342 [16] Pan, T.; Tutumluer, E.; Carpenter, S. (2006) Effect of coarse aggregate morphology on permanent
343 deformation behaviour of hot mix asphalt. *J Transp Eng-ASCE* 132, 580-589.
344 [https://doi.org/10.1061/\(ASCE\)0733-947X\(2006\)132:7\(580\)](https://doi.org/10.1061/(ASCE)0733-947X(2006)132:7(580)).
- 345 [17] Aragão, F.T.S.; Pazos, A.R.G.; Motta, L.M.G.D.; Kim, Y.-R.; Nascimento, L.A.H.D. (2016) Effects of
346 morphological characteristics of aggregate particles on the mechanical behaviour of bituminous paving
347 mixtures. *Constr Build Mater* 123, 444-453. <https://doi.org/10.1016/j.conbuildmat.2016.07.013>.
- 348 [18] Pei, J.; Bi, Y.; Zhang, J.; Li, R.; Liu, G. (2016) Impacts of aggregate geometrical features on the
349 rheological properties of asphalt mixtures during compaction and service stage. *Constr Build Mater* 126,
350 165-171. <https://doi.org/10.1016/j.conbuildmat.2016.09.033>.
- 351 [19] Sukhwani, R.; Little, D.; Masad, E. (2006) Sensitivity of HMA Performance to Aggregate Shape
352 Measured Using Conventional and Image Analysis Methods, TTI Report 0-1707-5. College Station,
353 Texas, 2006. <https://static.tti.tamu.edu/tti.tamu.edu/documents/0-1707-5.pdf>

- 354 [20] Zhang, D.; Huang, X.; Zhao, Y. (2012) Investigation of the shape, size, angularity and surface texture
355 properties of coarse aggregates. *Constr Build Mater* 34, 330-336.
356 <https://doi.org/10.1016/j.conbuildmat.2012.02.096>.
- 357 [21] Chen, J.-S.; Chang, M.; Lin, K. (2005) Influence of Coarse Aggregate Shape on the Strength of Asphalt
358 Concrete Mixtures. *Journal of the Eastern Asia Society for Transportation Studies* 6, 1062-1075.
359 <http://doi.org/10.11175/easts.6.1062>.
- 360 [22] Valdés-Vidal, G.; Calabi-Floody, A.; Miró-Recasens, M.; Norambuena-Contreras, J. (2015) Mechanical
361 Behaviour of asphalt mixtures with different aggregate type. *Constr Build Mater* 101, 474-481.
362 <https://doi.org/10.1016/j.conbuildmat.2015.10.050>.
- 363 [23] Valdés, G.; Miró, R.; Martínez, A.; Calabi, A. (2014) Effect of the physical properties of aggregates on
364 aggregate-asphalt bond measured using the UCL method. *Constr Build Mater* 73, 399-406.
365 <https://doi.org/10.1016/j.conbuildmat.2014.09.098>.
- 366 [24] Silva, H.M.R.D.; Oliveira, J.R.M.; Peralta, J.; Zoorob, S.E. (2010) Optimization of warm mix asphalts
367 using different blends of binders and synthetic paraffin wax contents. *Constr Build Mater* 24 [9], 1621-
368 1631. <https://doi.org/10.1016/j.conbuildmat.2010.02.030>.
- 369 [25] Valdés, G.; Pérez-Jiménez, F.; Martínez, A. (2012) Effect of temperature and asphalt mixture type on the
370 fatigue behaviour of flexible pavements. *Revista de la Construcción* 11 [1], 87-100.
371 <http://dx.doi.org/10.4067/S0718-915X2012000100009>.
- 372 [26] Kim, Y.R.; Kim, N.; Khosla, NP. (1992) Effects of Aggregate Type and Gradation on Fatigue and
373 Permanent Deformation of Asphalt Concrete. STP1147. ASTM International, (1992).
374 <https://doi.org/10.1520/STP24225S>.
- 375 [27] Kandhal P. S.; Parker F. J. (1998) Aggregate Tests Related to Asphalt Concrete Performance in
376 Pavements. National Cooperative Highway Research Program Report 405, Transportation Research
377 Board, National Research Council, Washington, D.C., (1998).
- 378 [28] Gonzalez, S. V.; Velandia, S. E. (2006) Estado del Arte en el Estudio de la Fatiga de Materiales
379 Bituminosos. Civil Engineering Thesis, Universidad Industrial Santander, Colombia.
- 380 [29] Moreno, F.; Rubio, M.C; Del Sol, M; Jiménez, A; Martínez, G; Martínez, M.J; Atienza, M; Quintana, L.;
381 Sierra, M.J.; Candau, J.; Sánchez, N. (2014) Influencia de Betunes Modificados en el Comportamiento

- 382 Mecánico de Mezclas Bituminosas. 7th Foro PTEC de Debate, La I+D+I en la Mejora de las
383 Infraestructuras del Transporte, Spain.
- 384 [30] Allen R. (2015) Chapter 10: Aggregates in Asphalt. The Shell Bitumen Handbook, ICE Publishing,
385 London. Pp. 217-259. ISBN: 978-0-7277-5837-8.
- 386 [31] Valdés Vidal G.; Calabi Floody A.; Norambuena-Contreras J.; Opazo A. (2015) Effect of aggregates
387 morphology and surface texture on the mechanical resistance of asphalt. 15th Congreso Internacional de
388 Metalurgia y Materiales CONAMET/SAM 2015, Chile. 17-20.

7. FIGURES

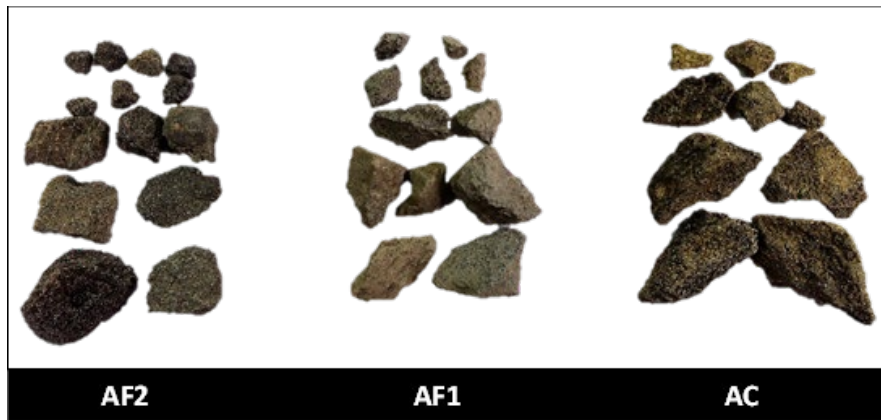


Fig. 1. Morphology of the aggregate used in this study.

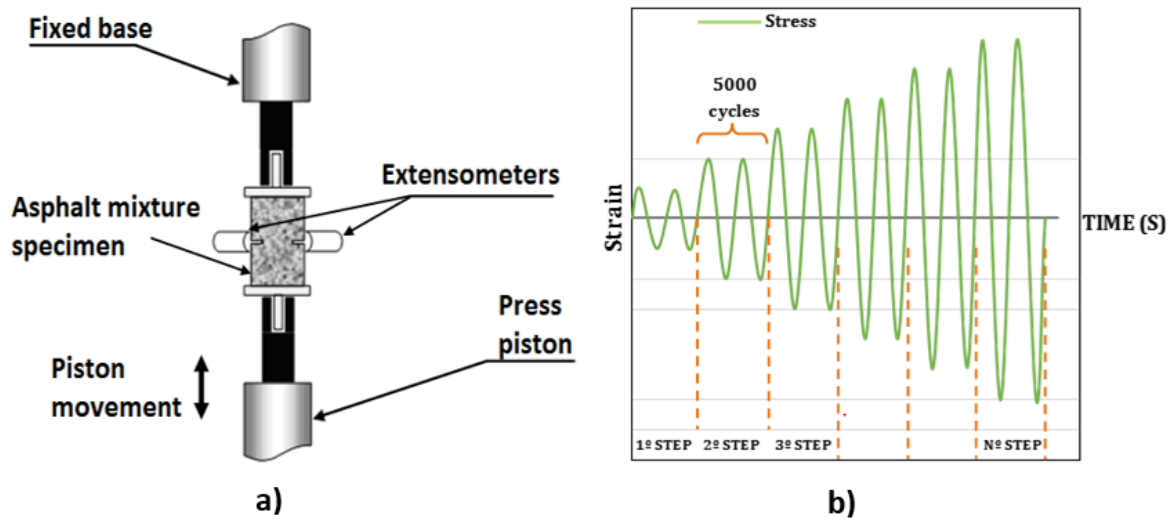


Fig. 2. a) EBADE Test device, b) sinusoidal strains tension-compression applied to the specimen.

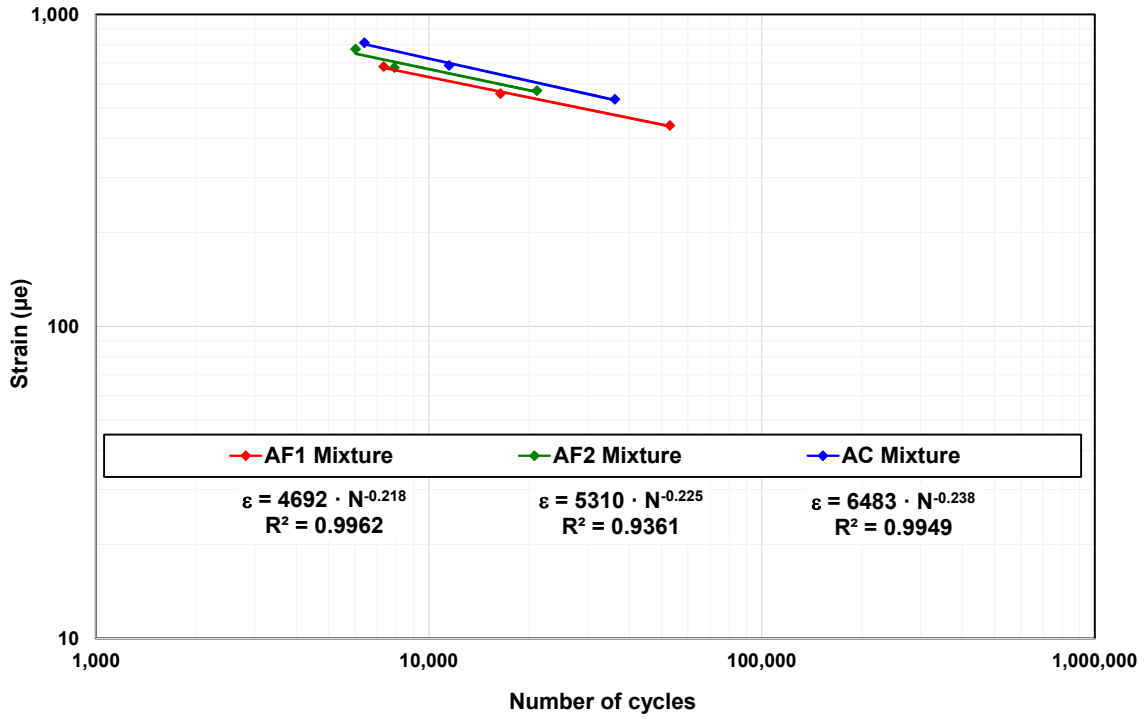


Fig. 3. Fatigue laws obtained through the fatigue indirect tensile test at 20°C.

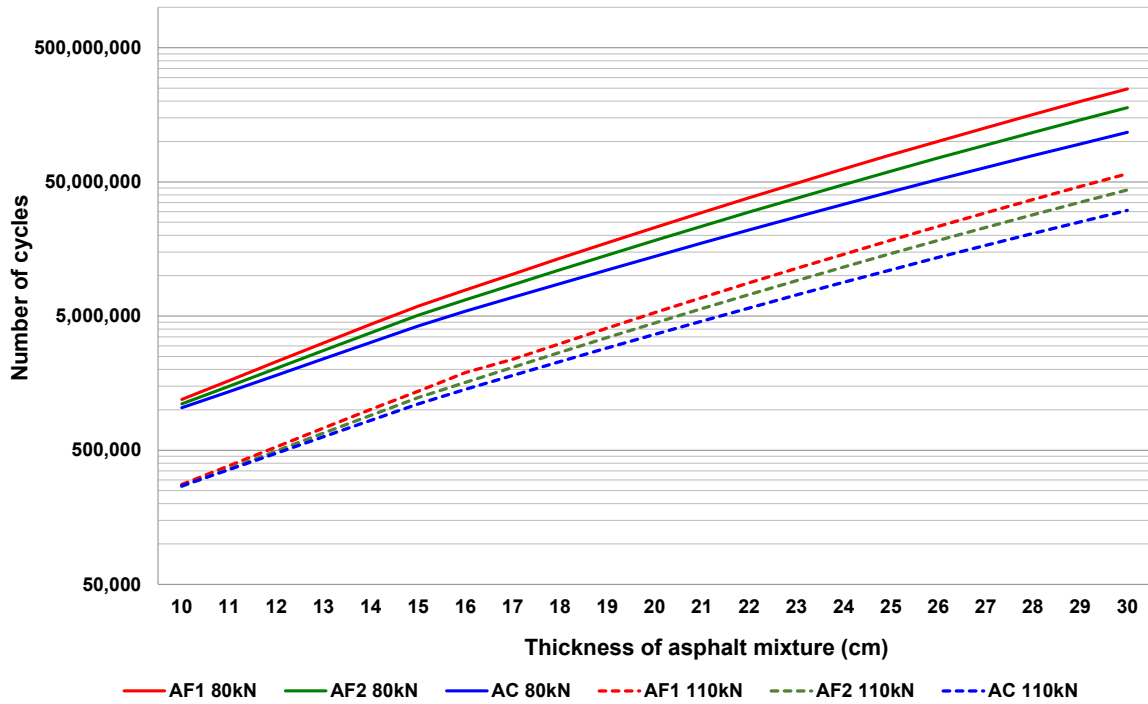


Fig. 4. Durability of the pavement structure for different thicknesses and traffic loads.

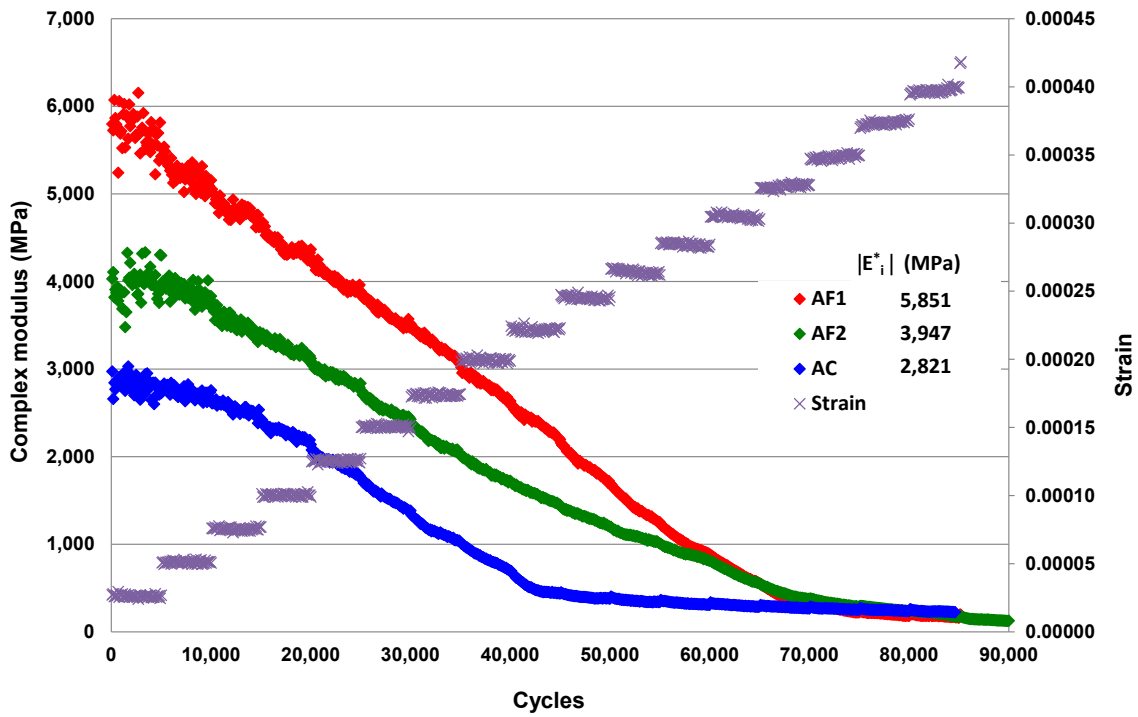


Fig. 5. Evolution of complex modulus in asphalt mixtures with different type of aggregates at 20°C.

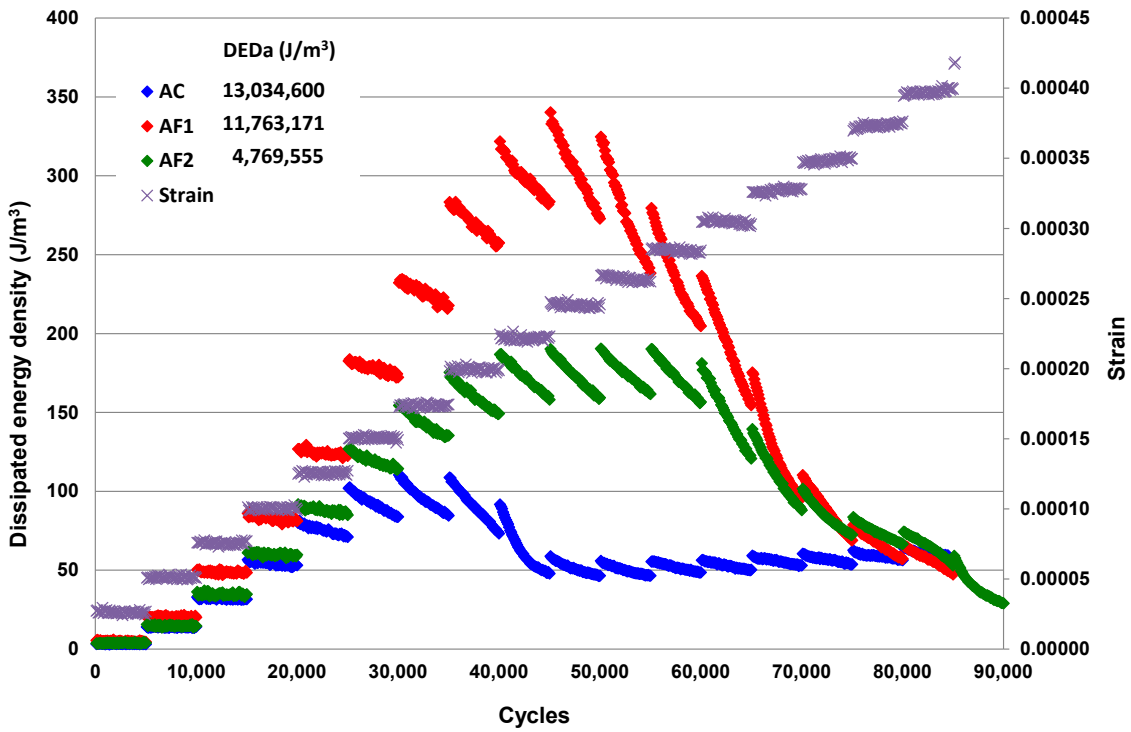


Fig. 6. Evolution of dissipated energy density in asphalt mixtures for different type of aggregates at 20°C.

8. TABLES

Table 1. Physical properties of binder.

Test	Standard method	Criteria	Test results
Absolute viscosity at 60°C, 300mmHg (P)	AASHTO – T202-80	Min 2400	3077
Penetration (dmm)	ASTM D36	Min 40	56
Ductility at 25°C (cm)	AASHTO T51	Min 100	>150
Softening point (°C)	ASTM D36-76	-	51
Flash point (°C)	AASHTO T48	Min 232	332
Trichloroethylene solubility (%)	AASHTO T44-78	-	99.9
Penetration index	-	-1.5 a +1.0	-0.7
RTFOT			
Mass loss (%)	AASHTO T240-13	Max 0.8	0
Absolute viscosity at 60°C, 300mmHg (P)	AASHTO – T202-80	-	7475
Ductility at 25°C (cm)	AASHTO T51	Min 100	150
Durability index	-	Max 3.5	2.4

Table 2. Physical properties of aggregates.

Tests	Specifications	AC	AF1	AF2
LA abrasion (%)	Máx.25%(*)-35%	25	16	15
Flakiness index (%)	Máx. 10%(*)-15%	8	2.5	0
Crushed aggregates (%)	Mín. 90(*)%-70%	100	92	90
Specific surface (m ² /kg)	-	36.34	31.15	31.24
Specific gravity (kg/m ³)	-	2360	2630	2640

(*) Wearing course

Table 3. Shape characterization parameters according to Zingg method.

Aggregate	Elongation Ratio*	Flatness Ratio *	Shape Factor *	Sphericity Factor *	Particle Shape
AF1	0.70	0.62	0.52	0.66	Disk
AF2	0.76	0.73	0.60	0.72	Cubical
AC	0.61	0.54	0.41	0.56	Blade

* Weighted according to the size proportion in the mixture.

Table 4. Particle index (PI) of aggregates used in the study.

Criterion type	Description	AC	AF1	AF2
Criterion I	All sizes are considered, according to their amount in the designed asphalt mixture.	14.3	16.8	14.1
Criterion II	Only coarse aggregate is considered (>2.5 mm), according to its amount in the designed asphalt mixture.	14.4	14.5	12.6
Criterion III	Only fine aggregate is considered (<2.5 mm), according to its amount in the designed asphalt mixture.	14.1	23.0	17.8

Table 5. IV-A-12 aggregate gradation.

Particle size, D (mm)	20	12.5	10	5	2.5	0.63	0.315	0.16	0.08	
Percent passing (%)	Max.	100	95	85	58	42	24	17	12	8
	Min.	100	80	70	43	28	13	8	6	4
	Selected gradation	100	92	81	55	30	15	10	7	5

Table 6. Average of durability in asphalt mixtures.

Thickness (cm)	ESALs of 80kN		ESALs of 110kN	
	Average AF1 vs AC (%)	Average AF1 vs AF2 (%)	Average AF1 vs AC (%)	Average AF1 vs AF2 (%)
10	13	7	2	3
15	29	14	20	11
20	39	20	31	16
25	47	24	40	21
30	53	28	47	24